Journal of Pharmaceutical Analysis 14 (2024) 101149

Contents lists available at ScienceDirect

Journal of Pharmaceutical Analysis

journal homepage: www.elsevier.com/locate/jpa

Original article

Depression of $Ca_V1.2$ activation and expression in mast cells ameliorates allergic inflammation diseases

Yongjing Zhang [a], Yingnan Zeng [a], Haoyun Bai [a], Wen Zhang [a], Zhuoyin Xue [a], Shiling Hu [a], Shemin Lu [b, c, **], Nan Wang [a, b, *]

[a] Department of Pharmaceutical Analysis, School of Pharmacy, Xi'an Jiaotong University, Xi'an, 710061, China
[b] Key Laboratory of Environment and Genes Related to Diseases (Xi'an Jiaotong University), Ministry of Education, Xi'an, 710061, China
[c] Department of Biochemistry and Molecular Biology, School of Basic Medical Sciences, Xi'an Jiaotong University, Xi'an, 710061, China

ARTICLE INFO

Article history:
Received 15 August 2024
Received in revised form
11 November 2024
Accepted 12 November 2024
Available online 14 November 2024

Keywords:
Allergy
Asthma
Mast cell
$Ca_V1.2$
CaMKII/PKC

ABSTRACT

Allergic inflammation is closely related to the activation of mast cells (MCs), which is regulated by its intracellular Ca^{2+} level, but the intake and effects of the intracellular Ca^{2+} remain unclear. The Ca^{2+} influx is controlled by members of Ca^{2+} channels, among which calcium voltage-gated channel subunit alpha1 C ($Ca_V1.2$) is the most robust. This study aimed to reveal the role and underlying mechanism of MC $Ca_V1.2$ in allergic inflammation. We found that $Ca_V1.2$ participated in MC activation and allergic inflammation. Nimodipine (Nim), as a strong $Ca_V1.2$-specific antagonist, ameliorated allergic inflammation in mice. Further, $Ca_V1.2$ activation in MC was triggered by phosphatizing at its Ser1928 through protein kinase C (PKC), which calcium/calmodulin-dependent protein kinase II (CaMKII) catalyzed. Overexpression or knockdown of MC $Ca_V1.2$ influenced MC activation. Importantly, $Ca_V1.2$ expression in MC had detrimental effects, while its deficiency ameliorated allergic pulmonary inflammation. Results provide novel insights into $Ca_V1.2$ function and a potential drug target for controlling allergic inflammation.

1. Introduction

Allergic diseases, including asthma [1], anaphylaxis [2], atopic dermatitis [3], and allergic rhinitis [4], have caused a substantial public health burden, reduced quality of life, and even led to premature death [5,6]. The pathophysiology of allergic diseases is dominated by IgE-mediated inflammation [7] and the type 2 immune response [8,9], and mast cells (MCs) play a pivotal role in the effective phase of allergic inflammation by releasing granules and cytokines [10]. Inflammation is the main symptom of allergic reactions; however, there is evident differences between allergy and inflammation [11]. Allergy is caused by exposure to antigens and other substances, marked by the activation of MCs [12]. Inflammation is a more broad-spectrum defense strategy to external stimuli. The current treatment for allergic diseases mainly focuses on relieving symptoms, and the drugs used are mostly histamine antagonists and corticosteroids [13]. Long-term use may cause side effects. It is urgently to discover new therapeutic targets and drugs.

MCs activation is triggered by the binding of high-affinity IgE receptor (FcεRI) with allergen-binding IgE [14] or by the activation of Mas-related G protein-coupled receptor-X2 (MrgX2) [15,16]. After the activation, cytoplasm calcium content significantly increases by both influx and release from the calcium pool [17]. Ca^{2+} mediates acute MC degranulation and delays the transcriptional production of cytokines, leukotrienes, and other secondary mediators [18]. The intercellular and extracellular Ca^{2+} flux is controlled by members of Ca^{2+} channels, such as Ca^{2+} release-activated Ca^{2+} (CRAC) [19], cell membrane transient receptor potential (TRP) [20,21], and calcium voltage-gated (Ca_V) channels [22,23]. At present, CRAC and TRP channels are recognized as the essential Ca^{2+} flux approach of MC [24,25], however, the absence of the above two channels cannot eliminate the Ca^{2+} influx during MC activation [26,27], indicating that there might be other Ca^{2+} channels to have participated in intracellular Ca^{2+} influx. As a rapid and efficient Ca^{2+} channel, $Ca_V1.2$ serves as the principal route of Ca^{2+} influx in many cells [28,29] and is also expressed on MC [23], but whether it is involved in MC activation and Ca^{2+} influx is unknown.

Peer review under responsibility of Xi'an Jiaotong University.
* Corresponding author. Department of Pharmaceutical analysis, School of Pharmacy, Xi'an Jiaotong University, Xi'an, 710061, China.
** Corresponding author. Department of Biochemistry and Molecular Biology, School of Basic Medical Sciences, Xi'an Jiaotong University, Xi'an, 710061, China.
E-mail addresses: wangnan2014@xjtu.edu.cn (N. Wang), lushemin@mail.xjtu.edu.cn (S. Lu).

https://doi.org/10.1016/j.jpha.2024.101149

$Ca_V1.2$, one of the major types of L-type Ca^{2+} channels, is composed of pores α subunits and regulation β and δ subunits, among which α subunit contains four main transmembrane domains [28]. Abnormal $Ca_V1.2$ functions lead to a variety of neurological [30], cardiovascular, muscular, and psychiatric disorders [31]. As a voltage-gated channel, $Ca_V1.2$ opens mainly depending on membrane potential depolarization [28,32], and it is also reported that protein kinase A (PKA) and protein kinase C (PKC) induced its C-terminus phosphorylation augmented $Ca_V1.2$ activity [33,34]. A recent study highlights the role of PKC-dependent $Ca_V1.2$ channel activation in T helper 2 (Th2) cell function and emphasizes the potential role of $Ca_V1.2$ in the treatment of allergic diseases [35]. However, little is known about $Ca_V1.2$ in MrgX2-related allergic inflammation and its mechanism in MC activation [29,36].

This study aimed to reveal the role and opening mechanism of MC $Ca_V1.2$ in allergic inflammation. MC $Ca_V1.2$, triggered by its Ser1928 phosphorylation rather than depolarization, leads to Ca^{2+} influx and degranulation in MCs. To our knowledge, this is the first time to report that $Ca_V1.2$ deficiency of MC could ameliorate allergic pulmonary inflammation. The results provide novel insights into understanding the role and underlying mechanism of $Ca_V1.2$, and expect a potential approach to intervene the allergic inflammatory diseases.

2. Materials and methods

2.1. Drug and reagents

Nimodipine (Nim), nicardipine, amlodipine, felodipine, nifedipine, and verapamil (all with a purity >98%) were obtained from the National Institutes for Food and Drug Control (Beijing, China). *p*-Nitrophenyl *N*-acetyl-β-D-glucosaminide, fluorescein isothiocyanate (FITC)-avidin, Evans blue, compound 48/80 (C48/80), and ovalbumin (OVA) were obtained from Sigma-Aldrich (St. Louis, MO, USA). House dust mite (HDM) was purchased from Greer Labs (Lenoir, NC, USA). Triton X-100 was obtained from Qingdao Meigao Chemical Co., Ltd. (Qingdao, China). Histamine-α,α,β,β-d4 dihydrochloride (purity 98%) was purchased from Cambridge Isotope Laboratories, Inc. (Tewksbury, MA, USA). Fluo-3-pentaacetoxymethyl ester (Fluo-3 AM) was obtained from Thermo Fisher Scientific Inc. (Waltham, MA, USA). Pluronic F-127 was procured from Biotium (San Francisco, CA, USA). StemPro-34 medium and human stem cell factors (SCFs) were obtained from Cell Signaling Technology, Inc. (Danvers, MA, USA). Human and mouse tumor necrosis factor (TNF)-α, C—C motif chemokine ligand 2 (CCL-2), and macrophage inflammatory protein (MIP) 2 enzyme-linked immunosorbent assay (ELISA) kits were bought from Sino Biological, Inc. (Beijing, China). ChamQ Universal SYBR qPCR Master Mix and HiScript III RT SuperMix for quantitative polymerase chain reaction (qPCR) (+genomic DNA (gDNA) wiper) were purchased from Vazyme (Nanjing, China).

Small interfering RNA (siRNA) was designed and synthesized by Genomeditech (Shanghai) Co., Ltd. (Shanghai, China). $Ca_V1.2$ expressing plasmid and cells were constructed using Procell (Wuhan, China). Primers for PCR were synthesized by Tianrun Aoke Biotechnology Co., Ltd. (Yangling, China).

Cluster of differentiation (CD) 117 (c-Kit) monoclonal antibody (2B8), phycoerythrin (PE), eBioscience™, and FceR1 alpha monoclonal antibody (MAR-1) FITC eBioscience™ (Thermo Fisher Scientific Inc.) were used in flow cytometry.

2.2. Animals and ethical statement

Six to eight-week-old female C57BL6 mice were purchased from the Experimental Animal Center of Xi'an Jiaotong University (Xi'an, China). The mice were fed standard dry chow twice a day with free access to water and housed in individual cages. The room temperature was 20—25 °C. The breeding environment was maintained a 12-h light/dark cycle, with a relative humidity of 40%. $Ca_V1.2^{fl/fl}$ mice were constructed using Cyagen Biosciences Inc. (Suzhou, China). Briefly, the *Cacna1c* gene (U.S. National Center for Biotechnology Information (NCBI) reference sequence: NM_001256002; Ensembl: ENSMUSG00000051331) is located on mouse chromosome 6. Forty-eight exons are identified, with the start codon (ATG) in exon 1 and the tag stop codon in exon 48 (transcript: ENSMUST00000112793). Exon 2 will be selected as the conditional knockout (CKO) region). Deletion of this region should result in the loss of function of the mouse *Cacna1c* gene. To engineer the targeting vector, homologous arms and (CKO) region will be generated by PCR using bacterial artificial chromosome (BAC) clone RP24-63D16 as template. Clustered regularly interspaced short palindromic repeats (CRISPR)-associated protein-9 nuclease (Cas9), gRNA, and targeting vector will be co-injected into fertilized eggs for CKO mouse production. The pups will be genotyped by PCR followed by sequencing analysis.

C57BL/6-Tg (*Cpa3-cre*) 4Glli/J (strain #:026828) was bought from the Jackson Laboratory (Bar Harbor, ME, USA) [37]. $Ca_V1.2^{fl/fl}Cpa3^{Cre/+}$ mice were obtained by crossing two types of mice and were identified by agarose gel electrophoresis.

This study was conducted in strict accordance with the recommendations of the Guide for the Care and Use of Laboratory Animals from the U.S. National Institutes of Health (NIH; Bethesda, Maryland, USA). The experimental protocol was approved by the Animals Ethics Committee of Xi'an Jiaotong University, Xi'an, China (Permit No.: XJTU 2019-711). All Animals were anesthetized with sodium pentobarbital.

2.3. Cell lines

Dr. Arnold Kirshenbaum and Dr. Dean Metcalfe (NIH) kindly provided laboratory of allergic diseases 2 (LAD2) human MCs. LAD2 was derived from the bone marrow of a 44-year-old male patient with macrocytosis and was established by the NIH Allergic Diseases Laboratory (Rockville, MD, USA). The cell line has been widely used in allergic disease studies. LAD2 cells were maintained at the 37 °C incubator containing 5% CO_2 and in the StemPro-34 medium containing 2 mM glutamine, 1:100 (*V*/*V*) penicillin-streptomycin (100 units/mL penicillin and 100 μg/mL streptomycin), and 100 ng/mL human SCF. The cells were maintained at a density of 2×10^6 cells/mL and the culture medium was replaced twice per week. $MrgX2^+$ cells (puromycin resistance) and $Ca_V1.2^+$ (ampicillin resistance) were constructed by lentivirus transfection and cultured in Dulbecco's modified eagle medium (DMEM) containing penicillin-streptomycin and 10% fetal bovine serum (FBS).

2.4. Bone marrow MC (BMMC) purification

Six to eight-week-old adult male C57BL/6 mice were sacrificed. The tibias were removed and were flushed by extensive rinsing with BMMC medium (Roswell Park Memorial Institute-1640 (RPMI-1640) medium, including 10% fetal serum, 0.07% β-mercaptoethanol, 1× penicillin-streptomycin, 2 mM L-glutamine, 10 mM hydroxyethyl piperazineethanesulfonic acid (HEPES), 100 ng/mL mouse SCF, and 20 ng/mL interleukin-3 (IL-3)). After centrifuging at 200 *g*, 5 min at room temperature, the cell pellet was collected and resuspended in BMMC medium. BMMCs were cultured for 4—6 weeks to complete differentiation.

2.5. Mouse peritoneal MC purification

Mice were sacrificed. Ice-cold MC dissociation media (MCDM) (Hanks' balanced salt solution (HBSS) with 10 mM HEPES, pH 7.2,

and 3% FBS) was used to make three sequential peritoneal lavages. Then the lavages were centrifuged at 4 °C, 200 *g* for 5 min. The cells were resuspended and layered over an isotonic 70% Percoll suspension (40 μL of 1 M HEPES, 320 μL of 10× HBSS, 830 μL of MCDM, and 2.8 mL of Percoll). Cells were collected after centrifugation. MCs were maintained at a concentration of 5×10^5 cells/mL in DMEM containing 10% FBS, 25 ng/mL recombinant SCF, and 100 U of penicillin-streptomycin.

2.6. MC identification by flow cytometry

Cells were collected and washed with phosphate-buffered saline (PBS), and then suspended with PBS containing 1% bovine serum albumin (BSA). PE-cyanine7-labeled anti-mouse-FCεRI antibodies and FITC-labeled anti-mouse-CD117 were added to label the cells. The mixture was then incubated at 4 °C for 45 min. Cell surface FCεRI and CD117 expression levels were detected using flow cytometry.

2.7. β-hexosaminidase release assay

LAD2 cells were pretreated with $Ca_V1.2$ inhibitors for 30 min and then stimulated with MrgX2 agonists for another 30 min. Cell supernatants and corresponding lysates were collected. LAD2 cells were seeded at 2.5×10^4 cells/well into a 96-well plate. The culture medium was removed, and C48/80 at 30 μg/mL in modified Tyrode's solution (120 mM NaCl, 2.5 mM $CaCl_2$, 4.7 mM KCl, 1.2 mM magnesium sulfate, 10 mM HEPES, 1.2 mM potassium dihydrogen phosphate, 5 mM BSA, and 5.5 mM glucose) was added to each well. 50 μL of supernatant of each well was transferred into other wells. Triton 1% (*V*/*V*) X-100 used for lysing cells. β-hexosaminidase activity was determined by incubating β-hexosamine with the cell lysate and supernatant.

2.8. Histamine release assay

An liquid chromatograph-mass spectrometer-8040 (Shimadzu, Kyoto, Japan) was used to detect histamine. The isocratic elution buffer was made up of acetonitrile water containing 0.1% formic acid and 20 mM ammonium formate (77:23, *V*/*V*) at a flow rate of 0.3 mL/min. Histamine was evaluated using a hydrophilic interaction liquid chromatography (HILIC) column (Venusil® HILIC, 2.1 mm × 150 mm, 3 μm, Agela Technologies, Tianjin, China).

2.9. Intracellular Ca^{2+} mobilization assay

$MrgX2^+$ and LAD2 cells were plated in a 96-well plate (1×10^4 cells/well) and incubated for 12 h at 37 °C. The cells were washed twice with calcium imaging buffer (CIB), 3 mM KCl, 125 mM NaCl, 0.6 mM $MgCl_2$, 2.5 mM $CaCl_2$, 10 mM HEPES, 1.2 mM $NaHCO_3$, 20 mM glucose, and 20 mM sucrose, pH adjusted to 7.4. The incubation buffer was made up of 0.1% (*m*/*V*) F-127 and 3.5 mM Fluo-3 AM, diluted with CIB at different concentrations of $Ca_V1.2$ inhibitors at 37 °C for 30 min. A total of 120 graphs (1 s per picture) of the cells were captured under blue light using a fluorescence microscope (Ti-U; Nikon, Tokyo, Japan).

2.10. Passive cutaneous anaphylaxis (PCA) model in mice

Adult male mice were randomly divided into the following groups (five mice per group): vehicle, and experimental groups (5, 10, and 20 mg/kg Nim orally administered). Nim was administrated 30 min before the C48/80 injection for one time. All the mice were anesthetized with 1% pentobarbital sodium and were intravenously injected with 0.2 mL of 0.4% Evans blue solution. Paw thickness was measured by a vernier caliper. Subsequently, 5 μL of C48/80 (30 μg/mL) was injected into the left paws. An equal volume of saline was injected into the right paw as a negative control (NC). 15 min after the injection, paw thickness was measured. The mice were photographed, and paw tissues were collected, dried for 24 h at 50 °C, and weighed. Evans blue was extracted the optical density was measured at 620 nm using a spectrophotometer (Bio-Rad, Hercules, CA, USA).

2.11. Body temperature

Mice were divided into different groups randomly. 30 min after gavage, C48/80 was injected through the tail veil. The body temperature of each mouse was measured using a biological function experimental system every 5 min for 30 min by inserting a probe into the anus of the mice.

2.12. Antigen-induced pulmonary inflammation in mice

OVA and HDM were used as antigens. Briefly, 8-week-old female C57BL/6 mice were sensitized with 0.5 mg/kg OVA intraperitoneally on days 1, 3, 5, and 7. Mice were placed in sealed containers and administered filtered 1% OVA for 30 min each time on days 21, 23, 25, 27, and 29 to induce asthma attacks. The mice in the vehicle group inhaled atomized PBS.

20 μg of HDM (10 μL) was administrated nasally for each mouse on days 1, 3, 5, and 7. Then 20 μg of HDM (10 μL) was administrated nasally to evoke pulmonary inflammation. The mice in the vehicle group inhaled atomized PBS.

2.13. MCs reconstruction in CKO mic

Wild type (WT) BMMCs were harvested and cultured in BMMC medium for 21 days for maturity in advance. Then CKO mice were sensitized with 0.5 mg/kg OVA intraperitoneally on days 1, 3, 5, and 7. 5×10^6 WT BMMC were injected into CKO mice through the tail vein. After one week, mice were placed in sealed containers and administered filtered 1% OVA for 30 min each time on days 21, 23, 25, 27, and 29.

2.14. Measurement of airway hyperreaction (AHR) in mice

Mice were anesthetized and ventilated. Lung function was detected by FlexiVent apparatus (SCIREQ, Montreal, Canada). Methacholine (Ach) (0−100 mg/mL) was atomized and inhaled by mice. Newtonian resistance (Rn), respiratory resistance (Rrs), resistance of the peripheral lung (G), and static compliance (Cst) values were determined.

2.15. Bronchoalveolar lavage fluid (BALF) collection

Mice were anesthetized and then BALF was collected by lavage of the lungs three times with saline (1 mL). Cells were collected and resuspended in 200 μL of Hank's solution. Cell numbers were evaluated by smeared and Diff-Quik staining. The supernatants from the BALF samples were collected. The proportion of different cell subtypes (eosinophils and neutrophils) was quantified by counting at least 200 cells per smear.

2.16. Lung histology

Mouse lungs were fixed in neutral-buffered formalin and then embedded in paraffin. 5-μm-thick sections were sliced and used to Masson's, hematoxylin and eosin (HE), or periodic acid-Schiff (PAS) trichrome stains. The collagen deposition, mucus production, and infiltrated cell counts were quantified.

2.17. Cytokine and chemokine measurements

Mouse IgE, Th2 cytokines levels in serum, and BALF were detected using ELISA kits.

2.18. Reverse transcription-qPCR (RT-qPCR)

LAD2 cells were pretreated with Nim or Ro 31-8220 (Ro) for 30 min and then stimulated with C48/80 for 8 h. The total cellular RNA of LAD2 cells was extracted. Subsequently, RT was performed to acquire complementary DNA (cDNA). Real-time qPCR was performed with 2 μL of cDNA and 18 μL of master mix in a CFX384 Real-Time PCR Detection System (Bio-Rad) in triplicate. The gene messenger RNA (mRNA) levels were expressed as cycle threshold (C_q) values, and the relative expression level of genes was calculated using formula $2^{-\Delta\Delta Cq}$. Primers were shown in Supplementary data.

2.19. Membrane potential detection

LAD2 cells were seeded in a 96-well plate. Moreover, FluoVolt™ dye, 1000× (component A), and 100× PowerLoad™ concentrate (component B) were mixed and suspended in 10 mL of CIB as an incubation buffer. The cells were incubated for 30 min. The FluoVolt™ loading solution was removed, and the cells were washed twice in CIB. Cells were captured under blue light using a fluorescence microscope (Ti-U; Nikon) to visualize membrane staining with FluoVolt™ dye. 10 μM valinomycin was used as a positive control, and treated cells for 30 min. Subsequently, KCl solution was added to depolarize the cells.

2.20. Western blotting

Total proteins from the untreated and treated LAD2 cells were extracted under an ice-cold condition. The cells were attached to a six-well plate containing rat tail collagen. After stimulation, the cell supernatant was removed immediately and the plate was placed in liquid nitrogen to retain the protein transient state. Proteins were separated on the gel using sodium dodecyl sulfate-polyacrylamide gel electrophoresis (SDS-PAGE) (Shaanxi Pioneer Biotech Co., Ltd., Xi'an, China). The separated proteins were separated on a 10% gel using SDS-PAGE. The proteins were transferred onto polyvinylidene fluoride membranes. The membranes were then incubated overnight at 4 °C with the following primary antibodies: anti-$Ca_V1.2$ (1:1000, #21774-1-AP), anti-phospho-$Ca_V1.2$ (1:1000, #PA5-106078), and anti-GAPDH (1:2000, #2118) were purchased from Cell Signaling Technology, Inc. Anti-PKC (1:2000, #ab181558), anti-phospho-PKC (1:2000, #ab109539), anti-calcium/calmodulin-dependent protein kinase II (CaMKII) (1:1000, #ab134041), and anti-phospho-CaMKII (1:2000, #ab171095) were from Abcam (Cambridge, MA, USA). After secondary antibody incubation, images of the developed blots were captured by a Lane 1D™ trans-illuminator (Beijing Creation Science Co., Ltd., Beijing, China).

2.21. Co-immunoprecipitation

LAD2 cells, with or without C48/80 treatment, were washed with cold PBS. Immunoprecipitation lysis buffer was then added to lyse the cells for 30 min on ice. The cell lysate was broken using ultrasonic waves to make the lysis more complete. Subsequently, 200–350 μL of lysate (containing 1–3 mg of total protein) was added to spin columns with end caps, and 2 μg of $Ca_V1.2$ antibodies was added to 300 μL of incubation buffer. IgG was used as a NC. The cells were then incubated overnight at 4 °C. Subsequently, 50 μL of resuspended protein A sepharose beads slurry was added to spin columns to precipitate immune complexes and incubated at 4 °C for 4 h. End caps were removed, and the complexes were washed five times. Spin columns were placed into new 1.5 mL Eppendorf tubes to collect the elution product. Elute buffer (40 μL) was added to the spin columns. The spin columns were centrifuged at 4 ℃ and 10,000 rpm for 1 min for elusion. Elution was repeated once, and the two times elusion were combined. Moreover, 10 μL of alkaline neutralization buffer and 23 μL of 5× sample buffer were added to the total elution product. Western blotting was performed to verify the presence of corresponding protein binding.

2.22. Statistical analysis

Data are presented as the mean ± standard error of mean (SEM) and were statistically analyzed using the Student's *t*-test (to compare two groups) and analysis of variance (ANOVA) (to compare three or more groups). Two-tailed tests were used for comparisons between two groups, and ANOVA test was used for multiple groups. SPSS Statistics 26.0 was used for analysis. Differences were considered to be significant at $^{*}P < 0.05$, $^{**}P < 0.01$, and $^{***}P < 0.001$.

3. Results

3.1. $Ca_V1.2$-specific antagonists inhibits MC activation dose-dependently in vitro

$Ca_V1.2$ was expressed in SK-N-SH cell (used as $Ca_V1.2$ positive cell) (Fig. S1A) and LAD2 cells (Fig. S1B). RNA sequencing screen also found $Ca_V1.2$ in LAD2 cells, with adenosine triphosphatases (ATPase) Na^+/K^+ transporting subunit α 1 as membrane protein control (Fig. S1C). BayK-8644, the $Ca_V1.2$ agonist, induced Ca^{2+} influx and we confirmed that $Ca_V1.2$ participated in MC Ca^{2+} related activation (Fig. S1D). Thus, $Ca_V1.2$ was selected for further research. Six specific $Ca_V1.2$ antagonists were used to investigate whether $Ca_V1.2$ participated in MC activation, we found that all the six antagonists showed inhibitory effect dose-dependently on C48/80 induced LAD2 cell β-hexosaminidase release (Fig. 1A). Among the six antagonists, the inhibitory effect of Nim was the most significant, for the half-maximal inhibitory concentration (IC_{50}) of Nim was the smallest (18.23 ± 1.12 μM). Cell Counting Kit-8 (CCK-8) assay revealed that Nim had little effect on LAD2 cells viability (Fig. 1B). Nim also significantly inhibited β-hexosaminidase release induced by C48/80, substance P (SP), ciprofloxacin (Cipro), and sinomenine (Sino) (Fig. 1C). Moreover, Nim could inhibit cytokines release such as TNF-α and CCL-2 in both LAD2 cells and murine peritoneal MCs (MPMCs) in a dose-dependent manner (Fig. 1D). Also, Ca^{2+} influx in both LAD2 cells and MPMCs induced by C48/80 was attenuated by Nim (Fig. 1E). At the same time, Nim also has a significant inhibitory effect on IgE induced degranulation of MCs. Nim inhibits the degranulation of LAD2 cells stimulated by biotinylated streptavidin after IgE pre-incubation (Fig. S1E).

3.2. Nim ameliorates pseudo-allergic reaction and antigen induced pulmonary inflammation (AIPI) in mice

Apart from MC activation *in vitro*, the inhibitory effect of Nim on pseudo-allergic reactions and AIPI was observed in mice. In PCA mice, Nim inhibited the increment in paw thickness and Evans blue extravasation in a dose-dependent manner (Fig. 2A). As granules in MC was evaluated by measuring fluorescence intensity after FITC-avidin staining [38], we also observed MC degranulation in the skin of mice paws. The nucleus was stained with 4',6-diamidino-2-phenylindole (DAPI) and showed blue color; while the granules were stained with FITC-avidin and present as green color. C48/80

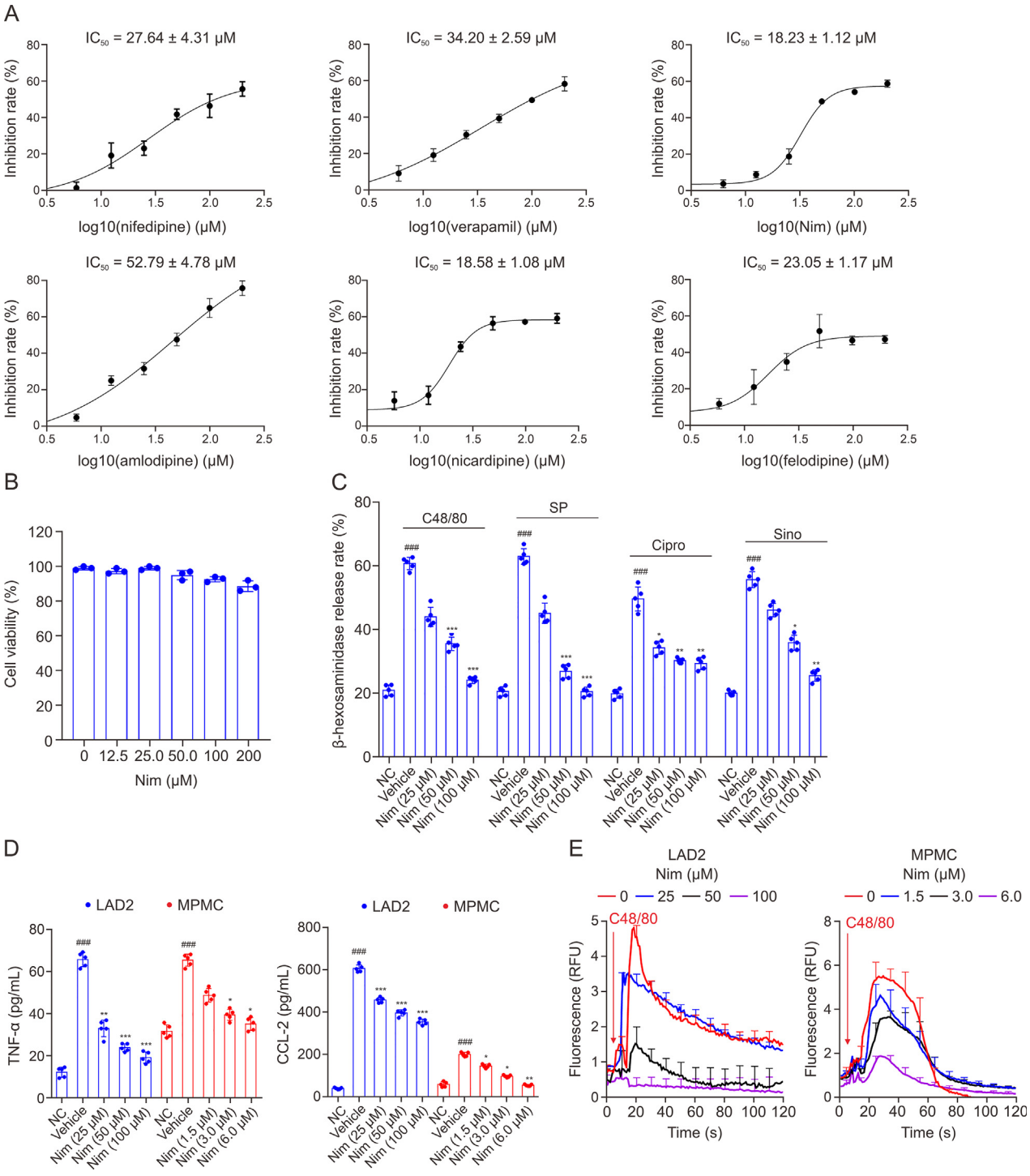

Fig. 1. The inhibitory effect of calcium voltage-gated channel subunit alpha1 C ($Ca_V1.2$) specific antagonists on mast cell (MC) activation *in vitro*. (A) The half-maximal inhibitory concentration (IC_{50}) of nicardipine, verapamil, nimodipine (Nim), amlodipine, nifedipine, and felodipine on β-hexosaminidase release in laboratory of allergic diseases 2 (LAD2) cells was detected. Among six $Ca_V1.2$ antagonists, Nim showed the best inhibitory effect, and the IC_{50} was 18.23 ± 1.12 μM. Hill value: nifedipine, 1.2731; verapamil, 0.7337; Nim, 3.3493; amlodipine, 0.7988; nicardipine: 3.6284; and felodipine, 2.4668. (B) LAD2 cell viability with Nim treatment. (C) The effect of Nim on MCs β-hexosaminidase release rate induced by various Mas-related G protein-coupled receptor-X2 (MrgX2) agonists: compound 48/80 (C48/80), substance P (SP), ciprofloxacin (Cipro), and sinomenine (Sino). (D) The effect of Nim on LAD2 cells and murine peritoneal MCs (MPMCs) release induced by C48/80. (E) The effect of Nim on LAD2 cells (left) and MPMCs (right) Ca^{2+} influx induced by C48/80. Experiments were repeated three times. Data are presented as the mean ± standard error of mean (SEM) and were analyzed using one-way analysis of variance (ANOVA) test. $^{*}P < 0.05$, $^{**}P < 0.01$, and $^{***}P < 0.001$, compared between experiment groups and vehicle; $^{\#\#\#}P < 0.001$, compared between experiment and negative control (NC) groups. TNF-α: tumor necrosis factor; CCL-2: C−C motif chemokine ligand 2; RFU: relative fluorescence unit.

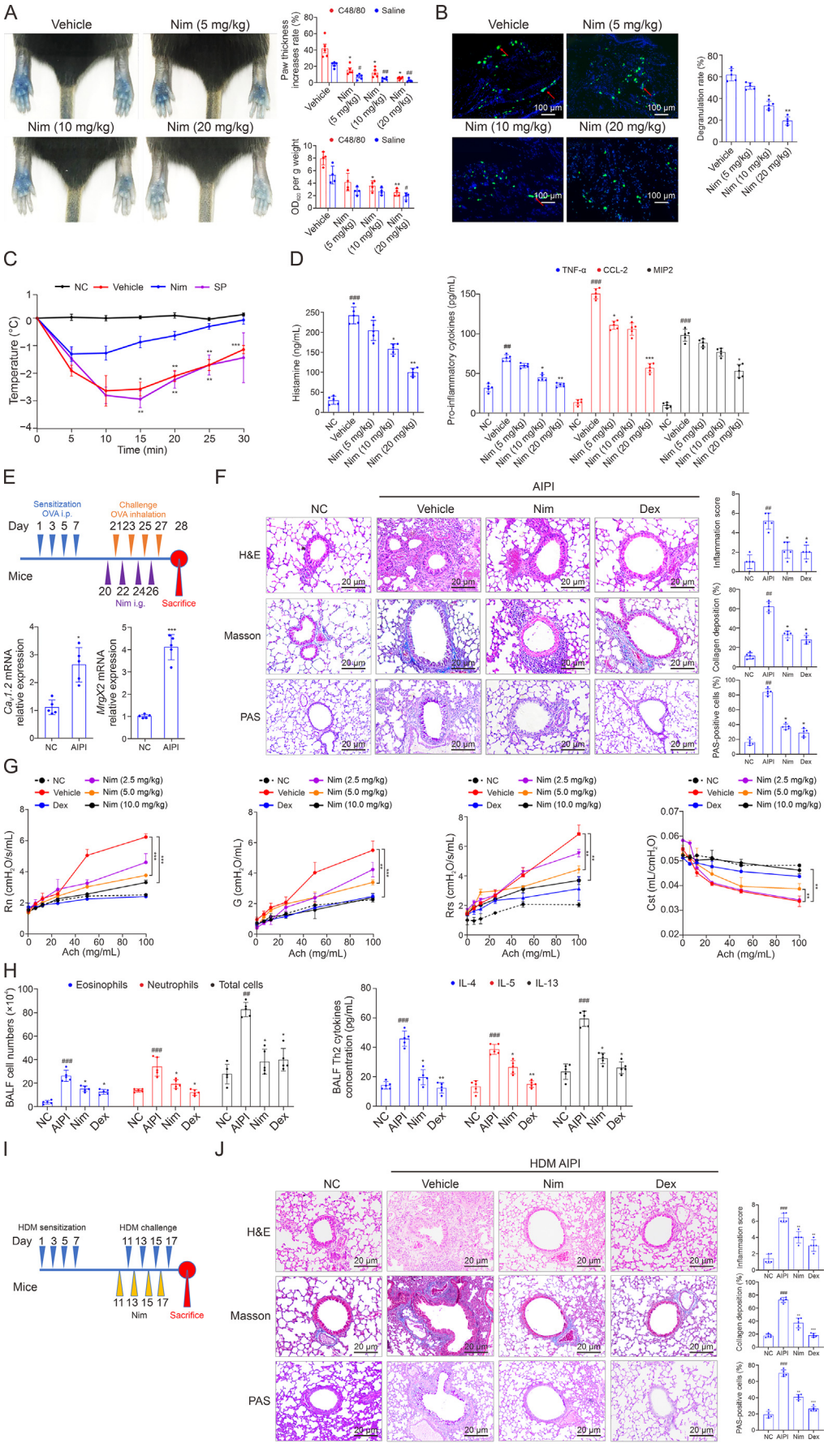
A
Vehicle
Nim (5 mg/kg)
Nim (10 mg/kg)
Nim (20 mg/kg)
C48/80
Saline
Paw thickness increases rate (%)
OD405 per g weight
B
Degranulation rate (%)
C
NC
Vehicle
Nim
SP
Temperature (°C)
Time (min)
D
Histamine (ng/mL)
TNF-α
CCL-2
MIP2
Pro-inflammatory cytokines (pg/mL)
E
Sensitization
OVA i.p.
Challenge
OVA inhalation
Day 1 3 5 7
2123 25 27 28
Mice
20 22 2426
Nim i.g.
Sacrifice
Ca1.2 mRNA relative expression
MrgX2 mRNA relative expression
F
AIPI
NC
Vehicle
Nim
Dex
H&E
Masson
PAS
Inflammation score
Collagen deposition (%)
PAS-positive cells (%)
G
Nim (2.5 mg/kg)
Nim (5.0 mg/kg)
Nim (10.0 mg/kg)
Rn (cmH2O/s/mL)
G (cmH2O/mL)
Rrs (cmH2O/s/mL)
Cst (mL/cmH2O)
Ach (mg/mL)
H
Eosinophils
Neutrophils
Total cells
BALF cell numbers (×10⁴)
IL-4
IL-5
IL-13
BALF Th2 cytokines concentration (pg/mL)
I
HDM sensitization
HDM challenge
Day 1 3 5 7
11 13 15 17
Mice
11 13 15 17
Nim
Sacrifice
J
HDM AIPI
NC
Vehicle
Nim
Dex
H&E
Masson
PAS
Inflammation score
Collagen deposition (%)
PAS-positive cells (%)

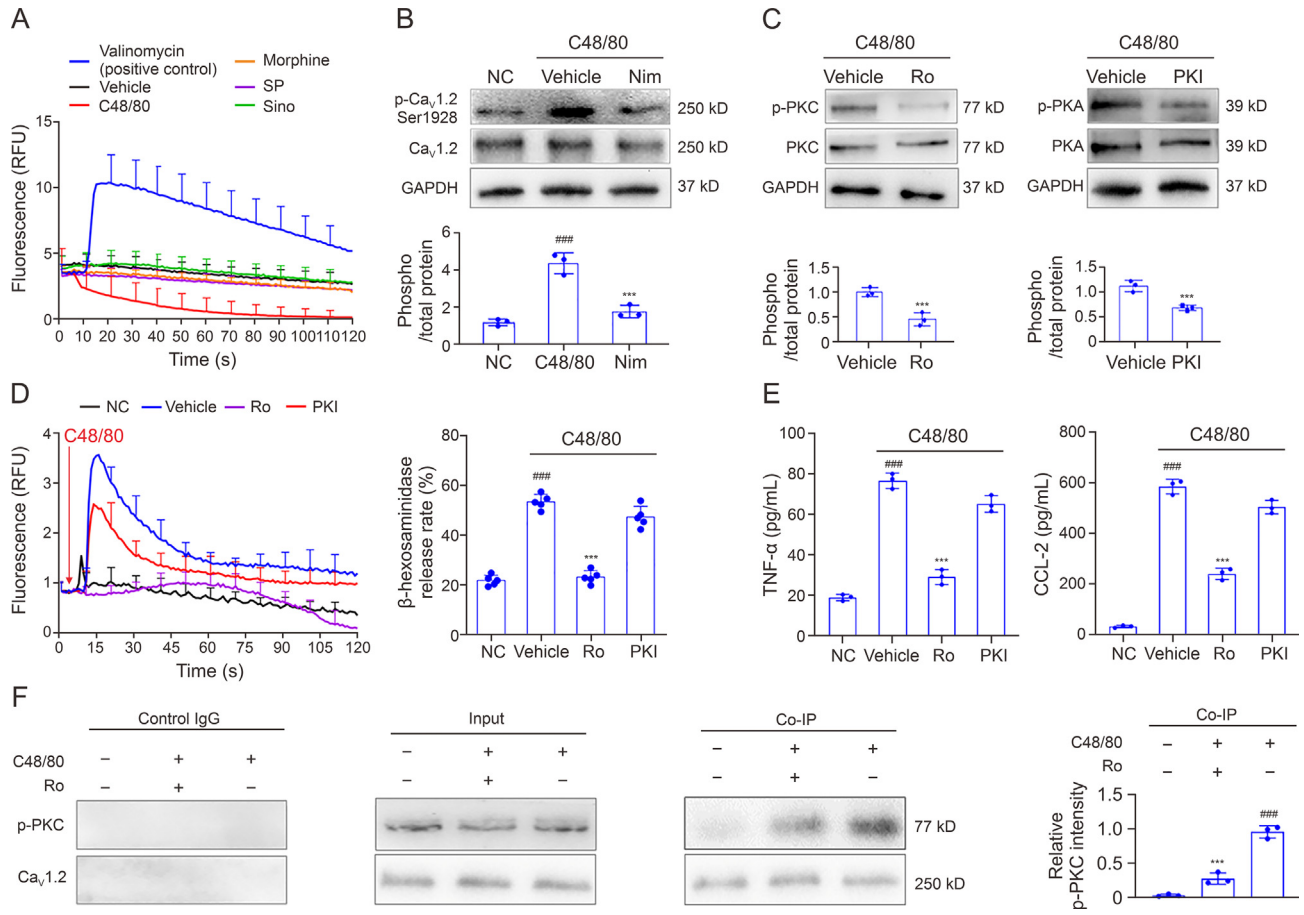

Fig. 3. Calcium voltage-gated channel subunit alpha1 C ($Ca_V1.2$) was activated by phosphorylating at Ser1928 through protein kinase C (PKC). (A) The membrane potential stimulated by different Mas-related G protein-coupled receptor X2 (MrgX2) agonists. (B) p-$Ca_V1.2$ at Ser1928 when induced by compound 48/80 (C48/80) and treated with nimodipine (Nim) in laboratory of allergic diseases 2 (LAD2) cells. (C) The phosphorylation of PKC and protein kinase A (PKA) induced by C48/80 and treated with Ro 31-8220 (Ro) (left) or PKA inhibitor (PKI) (right). (D) Ca^{2+} influx (left) and degranulation (right) in LAD2 cells treated with Ro or PKI. (E) Pro-inflammatory cytokines release in LAD2 cells treated with Ro or PKI. (F) Co-immunoprecipitation (Co-IP) displayed between p-PKC and $Ca_V1.2$ in C48/80 induced LAD2 cells (left) and the effect of Ro on the direct interaction (right). Experiments were repeated three times. Data are presented as the mean ± standard error of mean (SEM) and were analyzed using one-way analysis of variance (ANOVA) test. $^{***}P <$ 0.001, compared between experiment and vehicle or negative control (NC) groups; $^{\#\#\#}P < 0.001$, compared between experiment and NC groups. SP: substance P; Sino: sinomenine; RFU: relative fluorescence unit; GAPDH: glyceraldehyde 3-phosphate dehydrogenase; TNF-α: tumor necrosis factor; CCL-2: C–C motif chemokine ligand 2.

induced MC degranulation and the granules became diffuse, while granules remained steady in a dose-dependent manner after Nim administration (Fig. 2B). In addition, trypsin is another important sign of MC activation [39]. We found that the tail vein injection of C48/80 caused a significant increase in the content of trypsin in the serum of mice; However, the levels of tryptase in the serum of mice injected with C48/80 after Nim gavage were lower (Fig. S2). Furthermore, hypothermia is an important characteristic of allergic reaction [40]. In active systemic anaphylaxis (ASA) mice, the temperature of mice dropped dramatically at 5 min after C48/80 or SP injection. After another 5 min, the temperature decreased by 2.72 ± 0.67 °C while the temperature of mice pretreated with Nim only decreased by 1.22 ± 0.35 °C. Although mice temperature recovered at 30 min, the temperature of C48/80 or SP group was still about 1 °C lower than the initial temperature but Nim nearly reversed the decrease of temperature. (Fig. 2C). Furthermore, serum allergic mediator levels such as histamine, TNF-α, CCL-2, and MIP2, were also suppressed dose-dependently by Nim (Fig. 2D). Next, AIPI mice were induced by OVA inhalation and we found that $Ca_V1.2$ expression in lungs of AIPI mice was upregulated compared with normal mice (Fig. 2E). In addition, MrgB2, the MrgX2 homologue in mice and a biomarker of asthma [41], was also

Fig. 2. Nimodipine (Nim) ameliorated pseudo-allergic reaction and antigen induced pulmonary inflammation (AIPI) in mice. (A) The effect of Nim on mice paws increasement and exudation induced by compound 48/80 (C48/80). (B) Paw skin in different passive cutaneous anaphylaxis (PCA) groups was sliced and stained. The effect of Nim on PCA and mast cells (MCs) activation *in vivo* were quantified by paws swelling and the proportion of MCs with complete cell membrane structure. (C) The effect of Nim on C48/80 induced hypothermia in mice. (D) The effect of Nim on C48/80 induced histamine (left) and serum pro-inflammatory cytokines (right) release in active systemic anaphylaxis (ASA) mice serum. (E) Antigen induced pulmonary inflammation (AIPI) was induced by ovalbumin (OVA). Calcium voltage-gated channel subunit alpha1 C (*$Ca_V1.2$*, left) and Mas-related G protein-coupled receptor X2 (*MrgX2*, right) messenger RNA (mRNA) expression in AIPI mice. (F) Hematoxylin and eosin (H&E), Masson, and periodic acid-Schiff (PAS) stainings of lung sections in AIPI mice (left) and the effect of Nim on pulmonary inflammation (right). (G) Airway hyperresponsiveness of mice with different treatments. (H) T helper 2 (Th2) cytokine release and cell numbers in bronchoalveolar lavage fluid (BALF) of AIPI mice. (I) AIPI mice was induced by house dust mite (HDM). (J) H&E, Masson, and PAS stainings of lung sections in AIPI mice (left) and the effect of Nim on pulmonary inflammation (right). Experiments were repeated three times. Data are presented as the mean ± standard error of mean (SEM) and were analyzed using two-tailed unpaired Student's *t*-test or one way analysis of variance (ANOVA) test. $^{*}P < 0.05$, $^{**}P < 0.01$, and $^{***}P < 0.001$, compared between experiment groups and vehicle; $^{\#}P < 0.05$, $^{\#\#}P < 0.01$ and $^{\#\#\#}P < 0.001$, compared between experiment and negative control (NC) groups. SP: substance P; TNF-α: tumor necrosis factor; CCL-2: C–C motif chemokine ligand 2; MIP2: macrophage inflammatory protein 2; Dex: dexamethasone; Ach: acetylcholine; Rn: Newtonian resistance; G: resistance of the peripheral lung; Rrs: respiratory resistance; Cst: static compliance; IL: interleukin; PBS: phosphate-buffered saline.

overexpressed in AIPI mice lung (Fig. 2E), which indicating that $Ca_V1.2$ and MrgB2 may participate in allergic asthma. At the very beginning, Nim and dexamethasone (Dex) showed no significant effect on the lungs of mice without antigen sensitization stimulation such as OVA (Fig. S3). No obvious inflammatory infiltration, collagen deposition, and mucus secretion were observed in the lung tissue. Obvious airway remodeling, inflammatory cell infiltration, collagen deposition, and increased mucus secretion were presented in AIPI mice lungs, which were partially reversed by Nim (Fig. 2F). In the vehicle group, Ach induced severe AHR, including obvious increasing Rn, G, and Rrs and decreasing Cst. Mice AHR was attenuated by Nim treatment in a dose-dependent manner (Fig. 2G). The concentration of Th2 cytokines such as IL-4, IL-5, and IL-13 in BALF were decreased by Nim. Eosinophils, neutrophils, and total cell numbers in BALF were also decreased by Nim treatment (Fig. 2H). As a key indicator for evaluating allergic diseases, the levels of IgE in mouse serum were also tested. The results showed that Nim could only slightly reduce serum IgE levels while Dex significantly inhibited IgE levels (Fig. S4A). C48/80 injection did not induce IgE increase in mice serum (Fig. S4B). The above results showed that the anti-allergic effect of Nim may not be related to IgE. Apart from OVA, HDM was used to induce AIPI mice (Fig. 2I). HDM intranasally administration resulted in significant pathological changes in the lungs of mice, including inflammatory infiltration, collagen deposition, and mucus secretion. However, administration of Nim and Dex by gavage significantly relived the pathological changes in mice (Fig. 2J).

3.3. $Ca_V1.2$ is activated by phosphorylating at Ser1928 through PKC rather than depolarization

MC activators (C48/80, morphine, SP, and Sino) could not induce depolarization in LAD2 cells (Fig. 3A). We further found that when LAD2 cells were stimulated by C48/80, $Ca_V1.2$ was phosphorylated at

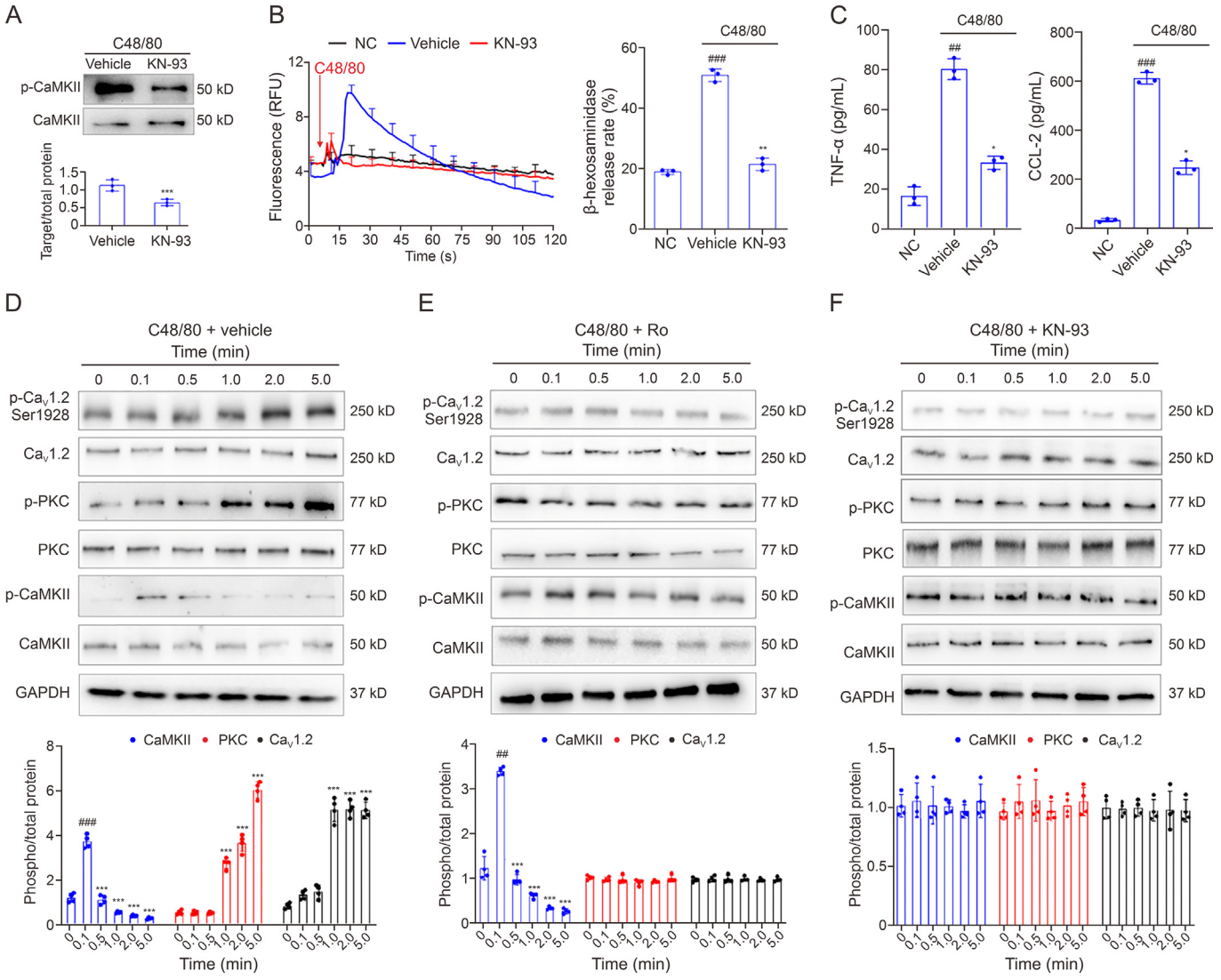

Fig. 4. Protein kinase C (PKC) activation was regulated by calcium/calmodulin-dependent kinase II (CaMKII) catalyzation. (A) The effect of KN-93 on the phosphorylation of CaMKII induced by compound 48/80 (C48/80). (B, C) The effect of KN-93 on Ca^{2+} influx (B, left), degranulation (B, right), and pro-inflammatory cytokines release (C) induced by C48/80 in laboratory of allergic diseases 2 (LAD2) cells. (D–F) Time series detection of CaMKII/PKC/ calcium voltage-gated channel subunit alpha1 C ($Ca_V1.2$) pathway: the phosphorylation of CaMKII, PKC, and $Ca_V1.2$ when Mas-related G protein-coupled receptor X2 (MrgX2) was activated (D), the effect of PKC inhibition on phosphorylation of CaMKII/PKC/$Ca_V1.2$ pathway (E), and the effect of CaMKII inhibition on phosphorylation of CaMKII/PKC/$Ca_V1.2$ pathway (F). Experiments were repeated three times. Data are presented as the mean ± standard error of mean (SEM) and were analyzed using one-way analysis of variance (ANOVA) test. $^{*}P < 0.05$, $^{**}P < 0.01$, and $^{***}P < 0.001$, compared between experiment and vehicle or negative control (NC) groups; $^{\#\#}P < 0.01$ and $^{\#\#\#}P < 0.001$, compared between experiment and NC groups. RFU: relative fluorescence unit; TNF-α: tumor necrosis factor; CCL-2: C–C motif chemokine ligand 2; GAPDH: glyceraldehyde 3-phosphate dehydrogenase.

Ser1928 (Fig. 3B). PKC inhibitor (Ro) and PKA inhibitor (PKI) were efficient in inhibiting MrgX2-induced PKC and PKA phosphorylation (Fig. 3C). β-hexosaminidase release and Ca^{2+} influx assays showed that Ro significantly suppressed MC activation, whereas PKI was not efficient, indicating that PKC, but not PKA, participated in MC activation (Fig. 3D). Same inhibitory effect was noticed in pro-inflammatory release (Fig. 3E). Importantly, based on our co-immunoprecipitation results, we found a direct interaction between PKC and $Ca_V1.2$ after C48/80 stimulation. We conducted quantitative statistics on the exposure intensity of *p*-PKC/$Ca_V1.2$ and found that there was a significant binding effect between $Ca_V1.2$ and *p*-PKC after C48/80 stimulation. Ro pre-treatment weakened the binding of the two proteins significantly (Fig. 3F).

3.4. MrgX2 causes sequential phosphorylation of CaMKII, PKC, and Ca_V12

KN-93, a CaMKII inhibitor, was used to inhibit the phosphorylation of CaMKII (Fig. 4A). It turned out that Ca^{2+} influx, cell degranulation, and pro-inflammatory cytokines release in LAD2 cells were inhibited by KN-93 (Figs. 4B and C). After treating primary BMMC cells with different inhibitors and then stimulating cells with C48/80, we found that KN-93 and Ro also inhibited BMMC activation violently while PKI showed slight inhibitory effect on Ca^{2+} influx, β-hexosaminidase release, and cytokines release (Fig. S5). Further mechanism study discovered that CaMKII was initially phosphorylated at 0.5 min approximately and then the phosphorylation of PKC (started at 1 min) and $Ca_V1.2$ (started at 1 min) occurred (Fig. 4D). While the phosphorylation of CaMKII was not influenced by PKC phosphorylation inhibition (Fig. 4E), the inhibitory of CaMKII phosphorylation suppressed PKC phosphorylation, indicating that CaMKII was the upstream of the pathway. The phosphorylation of CaMKII regulated the phosphorylation of PKC and $Ca_V1.2$ (Fig. 4F).

3.5. Manipulation of $Ca_V1.2$ expression influences function of MC and HEK293 cell

siRNA was used to knockdown $Ca_V1.2$ expression in MC (Fig. 5A). According to our results, Ca^{2+} influx and β-hexosaminidase release were reduced significantly when $Ca_V1.2$ was knockdown in LAD2 cells (Figs. 5B and C, and S6). We further expressed $Ca_V1.2$ in MrgX2 overexpressing HEK-293T cells ($MrgX2^+$) and obtained $MrgX2^+/Ca_V1.2^+$ cells (Fig. 5D). HEK293 cells without expressing MrgX2 and $Ca_V1.2$ were not activated by C48/80 from 1.87 to 15.0 μg/mL and was used as NC (Fig. 5E). We found that when C48/80 was 3.75 μg/mL, obvious Ca^{2+} influx was observed in $MrgX2^+/Ca_V1.2^+$ cells while

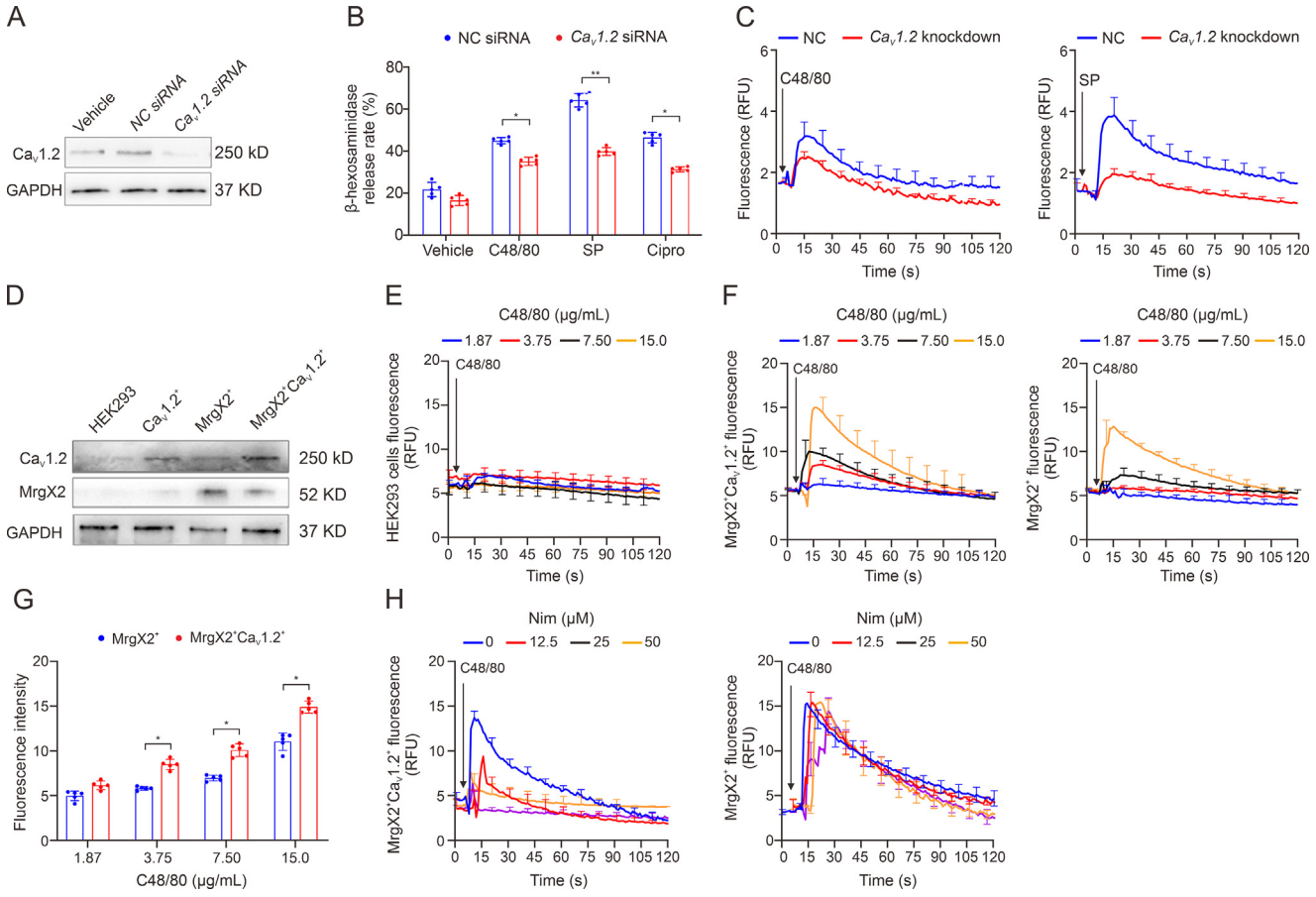

Fig. 5. Manipulation of calcium voltage-gated channel subunit alpha1 C ($Ca_V1.2$) expression influences function of mast cell (MC) and HEK293 cell. (A) $Ca_V1.2$ expression was knockdown by small interfering RNA (siRNA). (B) β-hexosaminidase release induced by compound 48/80 (C48/80), substance P (SP), and ciprofloxacin (Cipro) in $Ca_V1.2$ knockdown laboratory of allergic diseases 2 (LAD2) cells. (C) Ca^{2+} influx induced by C48/80 (left) or SP (right) was in $Ca_V1.2$ knockdown cells. (D) Mas-related G protein-coupled receptor-X2 $(MrgX2)^+$ cells and $MrgX2^+Ca_V1.2^+$ validation. (E) Ca^{2+} influx in HEK293 cells without MrgX2. (F) C48/80 induced Ca^{2+} influx in $MrgX2^+Ca_V1.2^+$ cells (left) and $MrgX2^+$ cells (right). (G) Fluorescence of Ca^{2+} in C48/80 induced $MrgX2^+Ca_V1.2^+$ cells and $MrgX2^+$ cells. (H) The effect of Nimodipine (Nim) on Ca^{2+} influx in $MrgX2^+Ca_V1.2^+$ cells (left) and $MrgX2^+$ cells (right). Experiments were repeated three times. Data are presented as the mean ± standard error of mean (SEM) and were analyzed using two-tailed unpaired Student's *t*-test and one-way analysis of variance (ANOVA) test. $^*P < 0.05$ and $^{**}P < 0.01$, compared between experiment groups and vehicle or HEK293. NC: negative control; GAPDH: glyceraldehyde 3-phosphate dehydrogenase; RFU: relative fluorescence unit.

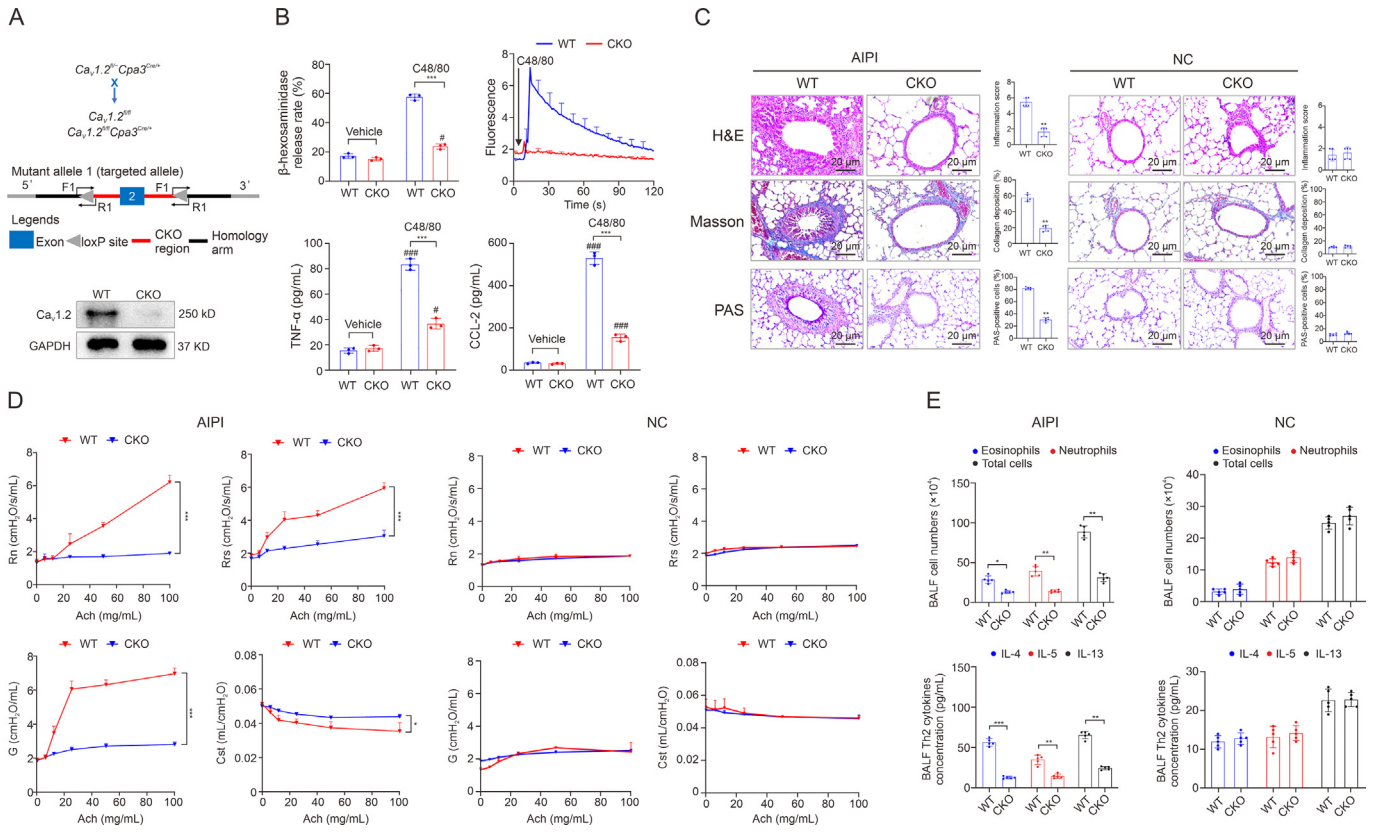

Fig. 6. Mast cell (MC)-specific deficiency of calcium voltage-gated channel subunit alpha1 C ($Ca_V1.2$) ameliorates the antigen induced pulmonary inflammation (AIPI). (A) Construction strategy and verification of conditional knockout (CKO) mice. (B) Bone marrow MCs (BMMCs) were isolated from $Ca_V1.2$ CKO mice and wild type (WT) mice. The effect of $Ca_V1.2$ knockout on MCs activation (degranulation, upper left; Ca^{2+} influx, upper right; cytokines release (bottom). (C) Hematoxylin and eosin (H&E), Masson, and periodic acid-Schiff (PAS) stainings of lung sections of $Ca_V1.2$ CKO mice and $Ca_V1.2^{fl/fl}$ mice (used as WT) in AIPI (left) and negative control (NC, right). (D) Airway hyperreaction (AHR) of CKO mice and WT mice in AIPI (left) and NC (right) groups. (E) The numbers of eosinophils, neutrophils, and total cells as well as T helper 2 (Th2) cytokines release in bronchoalveolar lavage fluid (BALF) in CKO and WT mice in AIPI (left) and NC (right) groups. Experiments were repeated three times. Data are presented as the mean ± standard error of mean (SEM) and were analyzed using one-way analysis of variance (ANOVA) test. $^{*}P < 0.05$, $^{**}P < 0.01$, and $^{***}P < 0.001$, compared between experiment and CKO or WT groups; $^{\#}P < 0.05$ and $^{\#\#\#}P < 0.001$, compared between experiment and WT groups. F1: forward primer 1; R1: reversed primer 1; loxP: locus of X (cross)-overinP1; GAPDH: glyceraldehyde 3-phosphate dehydrogenase; TNF-α: tumor necrosis factor; CCL-2: C–C motif chemokine ligand 2; Ach: acetylcholine; Rn: Newtonian resistance; Rrs: respiratory resistance; G: resistance of the peripheral lung; Cst: static compliance; IL: interleukin.

7.5 μg/mL C48/80 induced slight Ca^{2+} increase in $MrgX2^{+}$ cells. Above results revealed that the sensitivity of $MrgX2^{+}/Ca_V1.2^{+}$ cells to C48/80 was enhanced (Figs. 5F and G). At the same time, Nim had no inhibitory effect when $Ca_V1.2$ was absent in $MrgX2^{+}$ cells but inhibited Ca^{2+} influx in $MrgX2^{+}/Ca_V1.2^{+}$ cells (Fig. 5H).

3.6. MC-specific deficiency of $Ca_V1.2$ ameliorates MC activation and AIPI in mice

The genotyping strategies and breeding strategies of $Ca_V1.2$ CKO mice were displayed and $Ca_V1.2$ expression was abolished in CKO BMMCs, which demonstrated CKO mice was successfully established (Fig. 6A). Briefly, homozygous-targeted mice and $Cpa3^{Cre/+}$ mice were intercrossed to generate MC CKO mice and the selected CKO mice were marked in red blanks (Fig. S7A). We did not find significant difference in the development and reproduction of CKO mice compared to WT mice. Afterwards, BMMCs were isolated from $Ca_V1.2^{fl/fl}Cpa3^{Cre/+}$ (CKO) and $Ca_V1.2^{fl/fl}$ (WT) mice (BMMCs purity >90%) (Fig. S7B). When $Ca_V1.2$ was absent in CKO BMMC, Ca^{2+} influx, β-hexosaminidase release, and pro-inflammatory cytokines release were all decreased obviously (Fig. 6B). MC present in tissues both in WT mice and CKO mice. $Ca_V1.2$ was expressed on WT mice lung MCs (Fig. S7C). There was no significant difference in the number of MCs in the abdominal cavity and lung tissue between CKO mice and WT mice (Fig. S7D). CKO mice with AIPI showed little inflammatory cell infiltration, mucus secretion, and collagen deposition in lungs (Fig. 6C). Accordingly, the AHR, the numbers of eosinophils, neutrophils and total cells in BALF, as well as BALF Th2 cytokine content were lower in CKO mice than those in WT mice (Figs. 6D and E). Little pulmonary inflammation as well as AHR was observed in PBS-treated mice as NC. The above results preliminarily proved that the expression of $Ca_V1.2$ was related to the severity of airway inflammation.

3.7. Rescuing $Ca_V1.2$ expression exacerbates AIPI in CKO mice

To further investigate the effect of $Ca_V1.2$ on airway inflammation, CKO mice was replenished by WT BMMC. Specifically, the WT BMMC was injected into CKO mice through tail vein a week before OVA challenge (Fig. 7A). The cell numbers and proliferation rate of CKO and WT BMMCs in the induced environment (IL-3) was similar, and the cell density was similar (Fig. S7E). After WT BMMC transplantation, two kinds of MC exist in CKO mice, and the total number of MC was higher than that without transplantation (Fig. S7F). Airway inflammation and remodeling were rescued in CKO AIPI mice; however, after transplantation of WT BMMCs, mice showed obvious inflammatory cell infiltration, mucus secretion, and collagen deposition in lungs (Fig. 7B). AHR was partly regained in mice after received BMMC (Fig. 7C). Similarly, WT BMMCs transplantation regenerated Th2 cytokines release

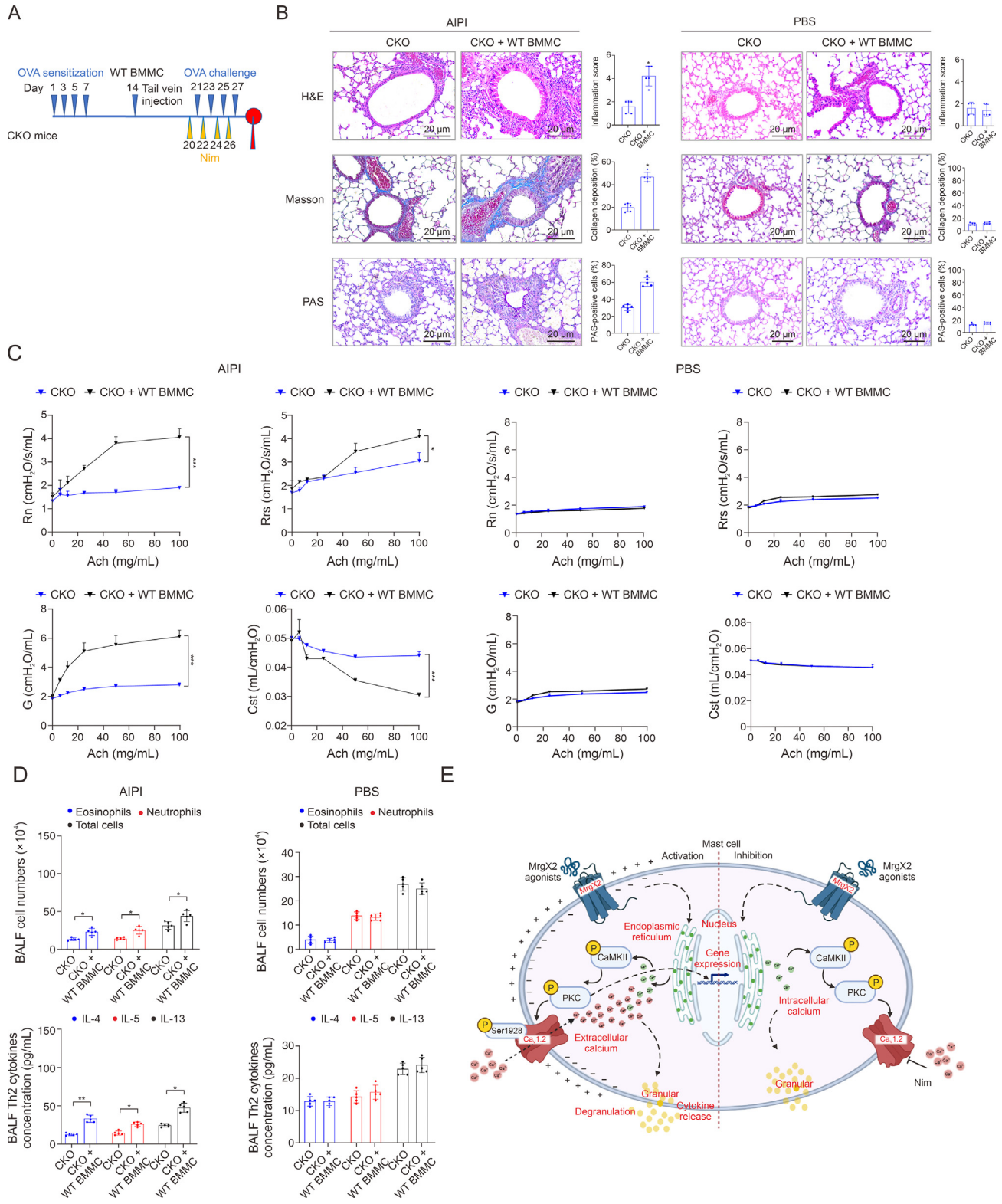

Fig. 7. Rescuing calcium voltage-gated channel subunit alpha1 C ($Ca_V1.2$) expression exacerbates antigen induced pulmonary inflammation (AIPI) in conditional knockout (CKO) mice. (A) CKO Mice received wild type (WT) bone marrow mast cells (BMMCs) transplantation and AIPI induction. (B) Hematoxylin and eosin (H&E), Masson, and periodic acid-Schiff (PAS) stainings of lung sections of CKO mice with or without WT BMMC transplantation in AIPI (left) or phosphate-buffered saline (PBS) (right) treatments. (C) Airway hyperreaction (AHR) of CKO mice with or without WT BMMC transplantation in AIPI (left) or PBS (right) treatments. (D) The numbers of eosinophils, neutrophils, and total cells as well as T helper 2 (Th2) cytokines release in bronchoalveolar lavage fluid (BALF) of CKO mice with or without WT BMMC transplantation in AIPI (left) or PBS (right) treatments. (E) $Ca_V1.2$ is involved in mast cell (MC) activation induced via Mas-related G protein-coupled receptor X2 (MrgX2). MrgX2 activation induced Ca^{2+} release from endoplasmic reticulum. Next, the intracellular Ca^{2+} activated calcium/calmodulin-dependent kinase II (CaMKII), which then phosphorylated protein kinase C (PKC). PKC phosphorylation interacted directly with $Ca_V1.2$ and caused Ser1928 phosphorylation, leading the opening of $Ca_V1.2$. Massive Ca^{2+} influx gave rise to MC activation. The $Ca_V1.2$ antagonists, including nimodipine (Nim), inhibited MC activation by inhibiting Ca^{2+} influx through $Ca_V1.2$. Experiments were repeated three times. Data are presented as the mean ± standard error of mean (SEM) and were analyzed using one-way analysis of variance (ANOVA) test. $^{*}P < 0.05$, $^{**}P < 0.01$, and $^{***}P < 0.001$. OVA: ovalbumin; Ach: acetylcholine; Rn: Newtonian resistance; Rrs: respiratory resistance; G: resistance of the peripheral lung; Cst: static compliance; IL: interleukin.

and cell numbers in BALF (Fig. 7D). As a control, little pulmonary inflammation was observed in PBS treated group (Figs. 7B and C). Similar to that of OVA, CKO mice showed little lung inflammation compared to WT mice induced by HDM (Fig. S8A). The IgE levels of each group of mice were detected and found that the serum IgE levels of CKO mice were similar to those of WT mice. At the same time, there was no significant change in IgE levels after WT BMMC transplantation (Fig. S8B). Fig. 7 clarified that when MC $Ca_V1.2$ was absent, the activation level of MC, pulmonary inflammation, and airway hyperresponsiveness were slight *in vivo* and *in vitro*; Fig. 7 showed the replenishment of WT MCs to CKO mice. The results showed that after replenishing WT MCs, the airway inflammation of CKO was recovered, which further proved that lung inflammation was related to the expression of MC $Ca_V1.2$. The above results verified that the presence of $Ca_V1.2$ in MCs was vital for the occurrence and development of pulmonary inflammation.

4. Discussion

In this study, we showed that $Ca_V1.2$ effectively participated in MC activation and pulmonary inflammation. The opening of $Ca_V1.2$ relied on its Ser1928 phosphorylation rather than cell membrane depolarization. Through the Cav1.2 activation, increasing intracellular calcium released the allergic mediators and transactivated the genes relevant to the MC cytokine (Fig. 7E). Importantly, CKO mice showed little pulmonary inflammation and AHR while CKO mice received WT BMMC redisplayed the symptoms (Fig. 7). $Ca_V1.2$ could be considered as a potential target for anti-allergic inflammation.

MrgX2 could be activated by multiple agonists and result in MC activation. The increase of intracellular Ca^{2+} concentration caused by Ca^{2+} influx leads to MC degranulation and inflammatory mediators release [42]. The current research focuses on CARC channels, mainly including IP3R, STIM1, and Orai1. These Ca^{2+} channels regulate Ca^{2+} influx to affect cell synthesis and release of inflammatory mediators, and have been used as anti-release targets for new drug design. In addition, L-type Ca^{2+} channels also form a part of MC Ca^{2+} channels; however, little was known about $Ca_V1.2$ in MC activated via MrgX2. As a type of Ca^{2+} channel with antagonists, $Ca_V1.2$ is expressed on the surface of MCs, but its activation and expression in MC activation and allergy have not been studied. Therefore, this study conducted in-depth research on the activation of $Ca_V1.2$ and its role in AIPI related to MrgX2. Our previous research confirmed that the crucial role of mitochondria in the activation process of MCs by disrupting mitochondrial oxidative respiration [13]. The results showed that MCs degranulation was inhibited without affecting normal mitochondrial activity. In our study, it was found out that Nim suppressed the MC activation induced by C48/80 (Fig. 1), indicating that MrgX2-mediated MC activation was related to $Ca_V1.2$. Further, $Ca_V1.2$ inhibition decreased Ca^{2+} influx and cytokines release in both human and mice MCs. Therefore, we assumed that $Ca_V1.2$ was involved in MC activation. We also used three *in vivo* models to evaluate the anti-allergic inflammation effect of Nim. *In vivo* FITC-avidin staining revealed that MC membrane was smooth and complete and contributed to the inhibitory effect of Nim (Fig. 2). Considering that MrgX2 (its mice homologue is MrgB2) [39] associated with asthma [41,43] and $Ca_V1.2$ were both overexpressed in lungs of AIPI mice, which were suppressed by Nim (Fig. 2), we believed that these two receptors may have mutual interaction in pulmonary inflammation. Nim, as a dihydropyridine Ca^{2+} antagonist, was used in clinic for cerebral vasospasm and ischemic hypertension with less adverse reactions [44]. It had a stronger inhibitory effect on MC activation, which has not been previously reported. Different stimulus, such as OVA/IgE or MrgX2 agonist (C48/80, SP, Sino, and Cipro) activate MCs via Ca^{2+}, thus the mechanism of Nim is consistent under different stimuli. Therefore, Nim could be used as an anti-allergic inflammation drug.

Since we confirmed that $Ca_V1.2$ in MC played a critical role in MC activation, we further investigated the opening mechanism of $Ca_V1.2$ in MC. $Ca_V1.2$ is a voltage gated ion channel, which is generally believed to be opened through membrane potential depolarization [28,32,45]. However, we found that the membrane potential of MC remained unchanged after MrgX2 activation for the first time (Fig. 3A). While $Ca_V1.2$ opening in IgE-mediated MC activation required depolarization [46], the specific reasons need further study. The phosphorylation of $Ca_V1.2$ Ser1928 was closely related to its activation, thus we studied the phosphorylation of $Ca_V1.2$ and found that Ser1928 of $Ca_V1.2$ was phosphorylated when MCs were activated and it was PKC rather than PKA participated in MC activation triggered by MrgX2 (Fig. 3). Furthermore, a direct interaction between PKC and $Ca_V1.2$ was observed (Fig. 3F). It is reported that the β subunit of $Ca_V1.2$ could also be phosphorylated and cause opening [47], which needs further research. It is reported that CaMKII controls PKC phosphorylation in many physiological activities such as oxidative stress [48] and apoptosis [49]. We found that CaMKII regulated PKC phosphorylation, and eventually led $Ca_V1.2$ Ser1928 phosphorylation in MC activation (Fig. 4). Meanwhile, we knocked down and knocked out MC $Ca_V1.2$. When $Ca_V1.2$ was knocked down, MC activation was partially inhibited, while $Ca_V1.2$ knockout immensely blocked the activation (Fig. 5). Although inhibition of the function and expression of $Ca_V1.2$ significantly impaired MC activity, Ca^{2+} influx and degranulation were not abolished completely, proving that other Ca^{2+} channels are involved.

Previous studies have confirmed that in rodent MC, it is most likely that $Ca_V1.2$ is involved in the Ca^{2+} influx after MC activation, rather than relying on the clearance of calcium storage in the endoplasmic reticulum [46]. At the same time, there are studies indicating that this $Ca_V1.2$ activation may be regulated by STIM1 [50], which is consistent with our findings on CaMKII activation. Whether internal calcium release [51] participated need further research. Interestingly, $Ca_V1.2$ overexpression led to a more sensitive Ca^{2+} influx to the stimulation, which may result from the rapid entry of Ca^{2+} mediated by $Ca_V1.2$, reaching the threshold earlier. Above all, $Ca_V1.2$ played a key role in MrgX2-mediated Ca^{2+} influx.

Considering that $Ca_V1.2$ is overexpressed in AIPI mice and Nim suppresses pulmonary inflammation, CKO mice were generated to evaluate the role of MC $Ca_V1.2$ in AIPI (Fig. 6). CKO mice showed normal basic physical indices without evident defects. MC present in tissues both in WT mice and CKO mice. There was no significant difference in the number of MCs in the abdominal cavity and lung tissue between CKO mice and WT mice, and the proliferation and survival rate of two cells were same, which provided a basis for our follow-up research (Fig. S7). Little pulmonary inflammation was observed in CKO AIPI mice. Importantly, CKO mice partly regained inflammation when received WT BMMC (Fig. 7). The above results strongly proved that $Ca_V1.2$ in MC participated in AIPI. Although the number of MC in the reconstructed mice increased, their pulmonary inflammatory symptoms and airway hyperresponsiveness were weaker than those in WT mice, which further demonstrated that $Ca_V1.2$ knockout MC could not cause pulmonary inflammation. The reason why CKO mice could not completely recover inflammation after transplantation may be that MC failed to participate in innate immune process of sensitization stage, which led to poor localization of immune cells [52]. The inhibitory effect of CKO was better than Nim, which was because antagonist was transient and reversible [53]. In summary, $Ca_V1.2$ could be a potential therapeutic target for allergic pulmonary inflammation.

It should be acknowledged that there are shortcomings in this article. Besides MCs, $Ca_V1.2$ is widely distributed in muscle cells. Therefore, the mechanism of Nim treatment on AHR may be related

to the relaxation of airway smooth muscle [54]. The gene edited cells and mice we constructed only involved the main structural alpha subunit of $Ca_V1.2$, while the role of other subunits of this receptor in allergies need further study [28]. Additionally, this study has not yet involved T cells that express $Ca_V1.2$ and play a significant role in AIPI [35,55,56].

5. Conclusion

In conclusion, our study demonstrates that $Ca_V1.2$ on MCs participates in pulmonary inflammation. The opening of $Ca_V1.2$ in MC activation occurred through the phosphorylation of its Ser1928 by PKC/CAMKII. Overall, $Ca_V1.2$ could be an allergic pulmonary inflammation target for drugs development. This study also provides new insights into understanding allergic inflammation and MC activation.

CRediT authorship contribution statement

Yongjing Zhang: Writing – review & editing, Writing – original draft, Methodology, Investigation, Formal analysis, Data curation, Conceptualization. **Yingnan Zeng:** Investigation, Formal analysis, Data curation, Conceptualization. **Haoyun Bai:** Methodology, Investigation, Formal analysis, Data curation. **Wen Zhang:** Investigation, Formal analysis. **Zhuoyin Xue:** Methodology, Investigation, Conceptualization. **Shiling Hu:** Visualization, Validation. **Shemin Lu:** Writing – review & editing, Supervision. **Nan Wang:** Writing – review & editing, Resources, Project administration, Funding acquisition, Conceptualization.

Declaration of competing interest

The authors declare that there are no conflicts of interest.

Acknowledgments

This work was funded by National Natural Science Foundation of China (Grant Nos.: 81930096 and 82274063). We thank Prof. Shengpeng Wang from Xi'an Jiaotong University for helpful review of the results, and Prof. Min Jia and Ms. Qiaohong Qin from Xi'an Medical University for their technical assistance in the airway responses detection.

Appendix A. Supplementary data

Supplementary data to this article can be found online at https://doi.org/10.1016/j.jpha.2024.101149.

References

[1] N. Akar-Ghibril, T. Casale, A. Custovic, et al., Allergic endotypes and phenotypes of asthma, J. Allergy Clin. Immunol. Pract. 8 (2020) 429–440.
[2] S.H. Sicherer, C.M. Warren, C. Dant, et al., Food allergy from infancy through adulthood, J. Allergy Clin. Immunol. Pract. 8 (2020) 1854–1864.
[3] S. Stander, Atopic dermatitis, N. Engl. J. Med. 384 (2021) 1136–1143.
[4] Y. Zhang, F. Lan, L. Zhang, Advances and highlights in allergic rhinitis, Allergy 76 (2021) 3383–3389.
[5] G.W.K. Wong, J. Li, Y.-X. Bao, et al., Pediatric allergy and immunology in China, Pediatr, Allergy Immunol. 29 (2018) 127–132.
[6] C.M. Warren, J. Jiang, R.S. Gupta, Epidemiology and burden of food allergy, Curr. Allergy Asthma Rep. 20 (2020), 6.
[7] M.H. Shamji, R. Valenta, T. Jardetzky, et al., The role of allergen-specific IgE, IgG and IgA in allergic disease, Allergy 76 (2021) 3627–3641.
[8] C.M. Lloyd, R.J. Snelgrove, Type 2 immunity: Expanding our view, Sci. Immunol. 3 (2018), eaat1604.
[9] W.W. Busse, M. Kraft, K.F. Rabe, et al., Understanding the key issues in the treatment of uncontrolled persistent asthma with type 2 inflammation, Eur. Respir. J. 58 (2021), 2003393.
[10] K. Amin, The role of mast cells in allergic inflammation, Respir. Med. 106 (2012) 9–14.
[11] J.A. Bellanti, R.A. Settipane, Allergy and immunology: at the crossroad of inflammation and disease, Allergy Asthma Proc. 44 (2023) 1–2.
[12] D. González-de-Olano, I. Álvarez-Twose, Mast cells as key players in allergy and inflammation, J. Investig. Allergol. Clin. Immunol. 28 (2018) 365–378.
[13] Y. Zhang, Z. Xue, S. Hu, et al., Chrysin inhibits pseudo-allergic reaction by suppressing mitochondrial STAT3 activation via MAS-related GPR family member X2, J. Agric. Food Chem. 69 (2021) 6569–6577.
[14] S.J. Galli, N. Gaudenzio, M. Tsai, Mast cells in inflammation and disease: Recent progress and ongoing concerns, Annu. Rev. Immunol. 38 (2020) 49–77.
[15] T. Plum, X. Wang, M. Rettel, et al., Human mast cell proteome reveals unique lineage, putative functions, and structural basis for cell ablation, Immunity 52 (2020) 404–416.e5.
[16] S. Roy, C. Chompunud Na Ayudhya, M. Thapaliya, et al., Multifaceted MRGPRX2: New insight into the role of mast cells in health and disease, J. Allergy Clin. Immunol. 148 (2021) 293–308.
[17] S. Feske, H. Wulff, E.Y. Skolnik, Ion channels in innate and adaptive immunity, Annu. Rev. Immunol. 33 (2015) 291–353.
[18] S. D'Costa, S. Ayyadurai, A.J. Gibson, et al., Mast cell corticotropin-releasing factor subtype 2 suppresses mast cell degranulation and limits the severity of anaphylaxis and stress-induced intestinal permeability, J. Allergy Clin. Immunol. 143 (2019) 1865–1877.e4.
[19] J. Di Capite, A.B. Parekh, CRAC channels and Ca^{2+} signaling in mast cells, Immunol. Rev. 231 (2009) 45–58.
[20] N. Serhan, L. Basso, R. Sibilano, et al., House dust mites activate nociceptor-mast cell clusters to drive type 2 skin inflammation, Nat. Immunol. 20 (2019) 1435–1443.
[21] M. Freichel, J. Almering, V. Tsvilovskyy, The role of TRP proteins in mast cells, Front. Immunol. 3 (2012), 150.
[22] Y. Suzuki, T. Yoshimaru, T. Inoue, et al., Ca v 1.2 L-type Ca^{2+} channel protects mast cells against activation-induced cell death by preventing mitochondrial integrity disruption, Mol. Immunol. 46 (2009) 2370–2380.
[23] Y. Suzuki, T. Inoue, C. Ra, Calcium signaling in mast cells: Focusing on L-type calcium channels, Adv. Exp. Med. Biol. 740 (2012) 955–977.
[24] I. Ashmole, P. Bradding, Ion channels regulating mast cell biology, Clin. Exp. Allergy 43 (2013) 491–502.
[25] S. Chaki, I. Alkanfari, S. Roy, et al., Inhibition of Orai channel function regulates mas-related G protein-coupled receptor-mediated responses in mast cells, Front. Immunol. 12 (2021), 803335.
[26] Y. Baba, K. Nishida, Y. Fujii, et al., Essential function for the calcium sensor STIM1 in mast cell activation and anaphylactic responses, Nat. Immunol. 9 (2008) 81–88.
[27] D. Zhang, A. Spielmann, L. Wang, et al., Mast-cell degranulation induced by physical stimuli involves the activation of transient-receptor-potential channel TRPV2, Physiol. Res. 61 (2012) 113–124.
[28] F. Hofmann, V. Flockerzi, S. Kahl, et al., L-type $Ca_V1.2$ calcium channels: From *in vitro* findings to *in vivo* function, Physiol. Rev. 94 (2014) 303–326.
[29] Y. Suzuki, T. Inoue, C. Ra, L-type Ca^{2+} channels: A new player in the regulation of Ca^{2+} signaling, cell activation and cell survival in immune cells, Mol. Immunol. 47 (2010) 640–648.
[30] Y. Li, H. Yang, T. He, et al., Post-translational modification of Cav1.2 and its role in neurodegenerative diseases, Front. Pharmacol. 12 (2021), 775087.
[31] G. Li, J. Wang, P. Liao, et al., Exclusion of alternative exon 33 of $Ca_V1.2$ calcium channels in heart is proarrhythmogenic, Proc. Natl. Acad. Sci. U S A 114 (2017) E4288–E4295.
[32] J. Isensee, M. van Cann, P. Despang, et al., Depolarization induces nociceptor sensitization by $Ca_V1.2$-mediated PKA-II activation, J. Cell Biol. 220 (2021), e202002083.
[33] T. Patriarchi, H. Qian, V. Di Biase, et al., Phosphorylation of Cav1.2 on S1928 uncouples the L-type Ca^{2+} channel from the β2 adrenergic receptor, EMBO J. 35 (2016) 1330–1345.
[34] D.H. Youn, S.F. Oliveria, M.L. Dell'Acqua, et al., Ser1928 is required for regulation of calcium-dependent inactivation of $Ca_V1.2$ L-type calcium channels by AKAP79-anchored PKA and calcineurin, Biophys. J. 102 (2012), 128a.
[35] V. Robert, E. Triffaux, P.E. Paulet, et al., Protein kinase C-dependent activation of $Ca_V1.2$ channels selectively controls human TH2-lymphocyte functions, J. Allergy Clin. Immunol. 133 (2014) 1175–1183.
[36] H. Chen, D.H. Vandorpe, X. Xie, et al., Disruption of Cav1.2-mediated signaling is a pathway for ketamine-induced pathology, Nat. Commun. 11 (2020), 4328.
[37] J.N. Lilla, C.-C. Chen, K. Mukai, et al., Reduced mast cell and basophil numbers and function in Cpa3-Cre; Mcl-1fl/fl mice, Blood 118 (2011) 6930–6938.
[38] M.D. Tharp, L.L. Seelig Jr., R.E. Tigelaar, et al., Conjugated avidin binds to mast cell granules, J. Histochem. Cytochem. 33 (1985) 27–32.
[39] J. Meixiong, M. Anderson, N. Limjunyawong, et al., Activation of mast-cell-expressed mas-related G-protein-coupled receptors drives non-histaminergic itch, Immunity 50 (2019) 1163–1171.e5.
[40] A. Nowak-Wegrzyn, M.C. Berin, S. Mehr, Food protein-induced enterocolitis syndrome, J. Allergy Clin. Immunol. Pract. 8 (2020) 24–35.
[41] N. Wang, J. Wang, Y. Zhang, et al., Imperatorin ameliorates mast cell-mediated allergic airway inflammation by inhibiting MRGPRX2 and CamKII/ERK signaling pathway, Biochem. Pharmacol. 184 (2021), 114401.
[42] C.R. Weiler, Mast cell activation syndrome: Tools for diagnosis and differential diagnosis, J. Allergy Clin. Immunol. Pract. 8 (2020) 498–506.

[43] J. An, J.H. Lee, H.K. Won, et al., Clinical significance of serum MRGPRX2 as a new biomarker in allergic asthma, Allergy 75 (2020) 959–962.
[44] A.P. Carlson, D. Hänggi, R.L. MacDonald, et al., Nimodipine reappraised: An old drug with a future, Curr. Neuropharmacol. 18 (2020) 65–82.
[45] E. Servili, M. Trus, J. Sajman, et al., Elevated basal transcription can underlie timothy channel association with autism related disorders, Prog. Neurobiol. 191 (2020), 101820.
[46] T. Yoshimaru, Y. Suzuki, T. Inoue, et al., L-type Ca^{2+} channels in mast cells: Activation by membrane depolarization and distinct roles in regulating mediator release from store-operated Ca^{2+} channels, Mol. Immunol. 46 (2009) 1267–1277.
[47] E. Servili, M. Trus, D. Maayan, et al., β-Subunit of the voltage-gated Ca^{2+} channel Cav1.2 drives signaling to the nucleus via H-Ras, Proc. Natl. Acad. Sci. U S A 115 (2018) E8624–E8633.
[48] B. Hegyi, J.M. Borst, L.R.J. Bailey, et al., Hyperglycemia regulates cardiac K^+ channels via O-GlcNAc-CaMKII and NOX2-ROS-PKC pathways, Basic Res. Cardiol. 115 (2020), 71.
[49] J.E. Kim, T.C. Kang, PKC, AKT and ERK1/2-mediated modulations of PARP1, NF-κB and PEA15 activities distinctly regulate regional specific astroglial responses following status epilepticus, Front. Mol. Neurosci. 12 (2019), 180.
[50] C.Y. Park, A. Shcheglovitov, R. Dolmetsch, The CRAC channel activator STIM1 binds and inhibits L-type voltage-gated calcium channels, Science 330 (2010) 101–105.
[51] C. Cao, H.J. Kang, I. Singh, et al., Structure, function and pharmacology of human itch GPCRs, Nature 600 (2021) 170–175.
[52] M. Sakata-Yanagimoto, T. Sakai, Y. Miyake, et al., Notch2 signaling is required for proper mast cell distribution and mucosal immunity in the intestine, Blood 117 (2011) 128–134.
[53] C. Türkeş, Y. Demir, Ş. Beydemir, Calcium channel blockers: Molecular docking and inhibition studies on carbonic anhydrase I and II isoenzymes, J. Biomol. Struct. Dyn. 39 (2021) 1672–1680.
[54] Z. Huang, Z. Qiu, L. Chen, et al., Cellular mechanism underlying the facilitation of contractile response induced by IL-25 in mouse tracheal smooth muscle, Am. J. Physiol. Lung Cell. Mol. Physiol. 323 (2022) L27–L36.
[55] J. Zeng, M. Li, Q. Zhao, et al., Small molecule inhibitors of RORγt for Th17 regulation in inflammatory and autoimmune diseases, J. Pharm. Anal. 13 (2023) 545–562.
[56] W. Zeng, Y. Song, R. Wang, et al., Neutrophil elastase: From mechanisms to therapeutic potential, J. Pharm. Anal. 13 (2023) 355–366.